

## Modelling and analysis of Virtual Coupling with dynamic safety margin considering risk factors in railway operations

Quaglietta, Egidio; Spartalis, Panagiotis; Wang, Meng; Goverde, Rob M.P.; van Koningsbruggen, Paul

**DOI**

[10.1016/j.jrtpm.2022.100313](https://doi.org/10.1016/j.jrtpm.2022.100313)

**Publication date**

2022

**Document Version**

Final published version

**Published in**

Journal of Rail Transport Planning and Management

**Citation (APA)**

Quaglietta, E., Spartalis, P., Wang, M., Goverde, R. M. P., & van Koningsbruggen, P. (2022). Modelling and analysis of Virtual Coupling with dynamic safety margin considering risk factors in railway operations. *Journal of Rail Transport Planning and Management*, 22, Article 100313. <https://doi.org/10.1016/j.jrtpm.2022.100313>

**Important note**

To cite this publication, please use the final published version (if applicable). Please check the document version above.

**Copyright**

Other than for strictly personal use, it is not permitted to download, forward or distribute the text or part of it, without the consent of the author(s) and/or copyright holder(s), unless the work is under an open content license such as Creative Commons.

**Takedown policy**

Please contact us and provide details if you believe this document breaches copyrights. We will remove access to the work immediately and investigate your claim.



ELSEVIER

Contents lists available at [ScienceDirect](https://www.sciencedirect.com)

## Journal of Rail Transport Planning &amp; Management

journal homepage: [www.elsevier.com/locate/jrtpm](http://www.elsevier.com/locate/jrtpm)

# Modelling and analysis of Virtual Coupling with dynamic safety margin considering risk factors in railway operations

Egidio Quaglietta<sup>a,\*</sup>, Panagiotis Spartalis<sup>b</sup>, Meng Wang<sup>c</sup>, Rob M.P. Goverde<sup>a</sup>, Paul van Koningsbruggen<sup>d</sup>

<sup>a</sup> Department of Transport & Planning, Delft University of Technology, 2628CN, Delft, the Netherlands

<sup>b</sup> Mott MacDonald, the Netherlands

<sup>c</sup> "Friedrich List" Faculty of Traffic and Transport Sciences, Technische Universität Dresden, Germany

<sup>d</sup> Technolution B.V., Gouda, the Netherlands

## ARTICLE INFO

## Keywords:

Virtual coupling  
Risk factors  
Dynamic safety margin  
Train following-model  
Capacity

## ABSTRACT

To address the ever-growing rail transport demand, the concept of Virtual Coupling train operations is gradually gaining ground within the railway industry. Thanks to a Vehicle-to-Vehicle communication, trains could be separated by less than an absolute braking distance and even form connected platoons to increase capacity at bottlenecks. However, a major concern about this concept regards the risk of safety violations in case of operational hazards pertaining to delays in train communication and control or emergency train stops. In this paper, the notion of dynamic safety margin is introduced for Virtual Coupling to dynamically adjust train separations so to always keep required safety distances also when hazardous operational events occur. The dynamic safety margin is embedded in a multi-state train-following model to analyse Virtual Coupling operations in presence of operational risk factors. A three-step methodology is applied in a real case study to fine-tune and verify the model, perform a sensitivity analysis, and identify capacity gains in several test scenarios including nominal and degraded traffic conditions. Results show that the use of a dynamic safety margin provides substantial capacity benefits to Virtual Coupling while respecting safe train distances even in case of sudden failures of the train control or communication systems. The notion of a dynamic safety margin can hence contribute to a safer version of Virtual Coupling operations and be considered by the railway industry in defining system requirements.

## 1. Introduction

Next-generation signalling technologies are being developed by the railway industry as potential solutions to address the need for an increased network capacity, while limiting costly and land-consuming infrastructure expansions. Train-centric signalling systems such as Moving block and Virtual Coupling are indeed major research topics on international research agendas such as the European Commission's [Shift2Rail Multi-Annual Actual Plan \(2015\)](#). Moving Block (MB) signalling ([Theeg and Vlasenko, 2014](#)) introduces a paradigm shift from traditional fixed-block railway operations by migrating vital equipment like signals and train detection devices from track-side to onboard. The need for apportioning tracks into sections is so removed, allowing train separation to be reduced from

\* Corresponding author.

E-mail address: [e.quaglietta@tudelft.nl](mailto:e.quaglietta@tudelft.nl) (E. Quaglietta).

<https://doi.org/10.1016/j.jrtpm.2022.100313>

Received 17 January 2022; Received in revised form 7 March 2022; Accepted 14 March 2022

Available online 17 March 2022

2210-9706/© 2022 The Authors. Published by Elsevier Ltd. This is an open access article under the CC BY license (<http://creativecommons.org/licenses/by/4.0/>).

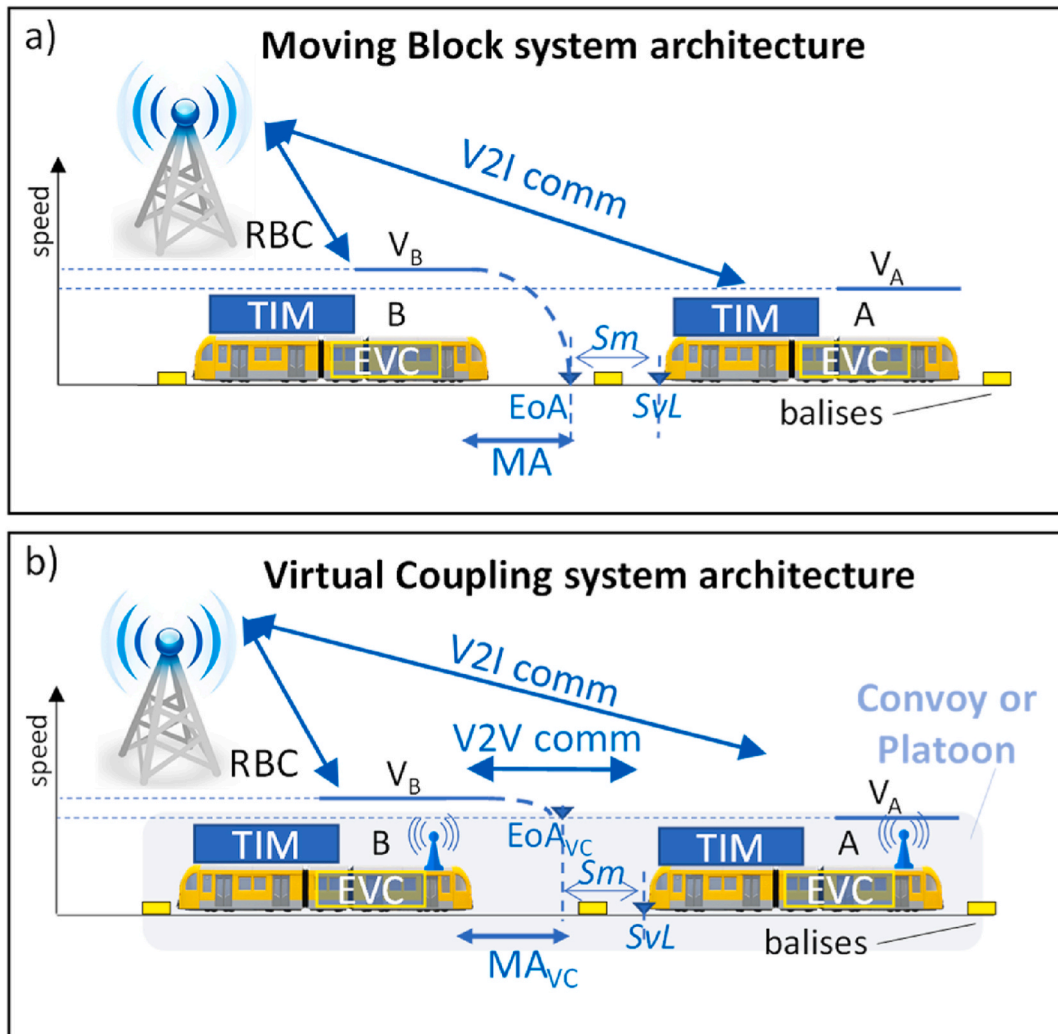


Fig. 1. Schematic system architecture for Moving Block ETCS Level 3 and Virtual Coupling.

a given number of blocks (depending on the amount of signal aspects) to the distance necessary for a train to reach a standstill from the current speed (i.e., the absolute braking distance). Virtual Coupling (VC) is a concept that advances MB signalling by relying on the assumption that train separation can be further reduced to less than an absolute braking distance if trains communicate with each other via a Vehicle-to-Vehicle (V2V) radio layer. Trains can hence form so-called “convoys” following each other at a relative braking distance as function of their speed differential or even travel in “platoons” where they move synchronously at a short margin from each other. Cooperative automatic train operation is deemed necessary in this case since the relative long human driving reaction times would prevent such short separations between trains.

While the implementation of MB mainly depends on a reliable Train Integrity Monitoring (TIM) and accurate train positioning, the deployment of VC also requires a clearer understanding of the trade-offs between safety implications and capacity benefits. Research performed so far (e.g., MOVINGRAIL, 2020; Quaglietta et al., 2020; Duan and Schmid, 2018) shows that VC provides only marginal capacity improvements at junctions, whereas substantial gains over MB are mostly obtained on plain tracks. Those studies are however based on nominal VC operational conditions assuming homogeneous rolling stock and neglecting relevant risk factors in real-life operations like: V2V communication delays, extended driving reaction times, train positioning errors and emergency braking applications during platooning. When considering those factors, the train separation under Virtual Coupling needs to be increased by additional safety margins to remove any safety risk arising from their individual or combined presence. This safety-critical increase in the VC train separation could consequently result in lower capacity improvements than those reported in literature. It is hence legit to ask whether in real rail operations, where the mentioned risk factors are commonplace, Virtual Coupling would still provide enough capacity gains over MB. The railway industry urges a concrete answer to this question to justify strategic investments for the development of Virtual Coupling.

This paper has the objective of providing a comparative capacity analysis between Virtual Coupling and Moving Block when

considering a realistic railway operation environment that features the presence of technological, and operational risk factors. The analysis relies on the Virtual Coupling multi-state train-following model by Quaglietta et al. (2020), which has been extended with a dynamic safety margin, specifically defined to mitigate different risk factors in real-life operations. The extended train-following model has been embedded in the microscopic railway simulation tool EGTRAIN to accurately assess capacity of VC and MB at different locations of a railway corridor. Results have been obtained by applying the model to part of the South West Main Line (SWML) in the UK.

The paper brings several main contributions to the current state-of-the-art on Virtual Coupling rail operations by:

- i) Introducing the concept of a dynamic safety margin for Virtual Coupling which accounts for train communication delays, positioning errors, driving reaction times, heterogeneous train braking characteristics, and emergency train braking applications.
- ii) Performing a sensitivity analysis of railway capacity to different Virtual Coupling risk factors existing in real-life rail operations as well as to track gradients, which can also play a role in the safe distancing of trains in a VC convoy or platoon.
- iii) Illustrating dynamic effects on train separation of convoys/platooning operations by simulating the interactions between multiple trains running under Virtual Coupling.
- iv) Identifying preliminary operational and technological configurations which can be useful to the railway industry for defining safe and capacity-effective VC signalling.

In Section 2 a literature review is provided on train-centric signalling systems and models describing Virtual Coupling operations. Section 3 illustrates the methodology applied while Section 4 describes the case study. Results are provided in Section 5, while Section 6 concludes the paper providing recommendations and future research directions.

## 2. Literature review on Virtual Coupling railway operations

### 2.1. Virtual Coupling signalling scheme

Virtual Coupling signalling advances the concept of moving-block railway operations, allowing trains to be separated by a relative braking distance rather than by an absolute braking distance.

Fig. 1 illustrates a schematic system architecture for Moving Block (a) and Virtual Coupling (b) signalling. In this paper we refer to the moving-block implementation of the European signalling standard ETCS Level 3 (Theeg and Vlasenko, 2009), where vital track-side train detection and line-side signals are totally replaced by on-board devices such as Train Integrity Monitoring (TIM), the European Vital Computer (EVC), and a Driver-Machine Interface (DMI). TIM continuously checks that no car is accidentally split from the trainset. Trains have a radio-based Vehicle-to-Infrastructure (V2I) communication with the Radio-Block Centre (RBC) reporting train position updates every few seconds (usually every 1–5 s). In return the RBC provides each train with a Movement Authority (MA) providing the maximum distance that a train can safely cross without colliding with another train on the route.

Train location is continuously monitored by the EVC by means of an on-board odometer which is regularly re-calibrated any time the train crosses a track-side transponder (named Eurobalise) acting as a fixed geographical reference point.

The MA is given as an encrypted message containing the last safe location until which the train can move, namely the End of Authority (EoA). The EoA is at a safety margin ( $s_m$ ) from the Supervised Location (SvL) which represents a potential danger on the train route such as the front or the tail of a nearby train, a speed or track access restriction and/or an unset switch. The safety margin  $s_m$  depends in turn on the train positioning error which is considered to increase linearly (with a 5% slope) from the position of the last crossed balise group. The EVC elaborates MA messages to compute and supervise in real-time a dynamic speed profile including a braking curve ensuring that the train does not overrun the EoA.

In this paper we refer to the Virtual Coupling signalling scheme sketched in the EU project MOVINGRAIL (2020), which builds on the Moving Block architecture and adds a V2V communication layer with corresponding onboard antennas to let trains exchange route and kinematic information (e.g., acceleration, speed). The type and format of messages exchanged via the V2I and the V2V communication layers are not yet specified for Virtual Coupling. The analysis hence refers to the train messaging flow described in Quaglietta et al. (2020), where the standard ETCS Movement Authority is upgraded to a Virtual Coupling Movement Authority ( $MA_{VC}$ ). The  $MA_{VC}$  combines the information of the RBC and the V2V channel to provide the trains with the maximum safe crossable distance as well as speed, acceleration and route of neighbouring trains. The end of  $MA_{VC}$  is called Virtual Coupling End of Authority ( $EoA_{VC}$ ) which, like a standard ETCS LoA (Limit of Authority), has an associated target speed that can be higher than 0. The speed associated to the  $EoA_{VC}$  is the speed of the train ahead (i.e.,  $V_A$  in Fig. 1) if trains are moving under Virtual Coupling, and it is 0 if the trains are decoupling (e.g., for a diverging junction that still has to be set). In this latter case The  $EoA_{VC}$  coincides with the standard EoA. To enable Virtual Coupling operations, the EVC is assumed to supervise both the  $EoA_{VC}$  and the standard ETCS EoA (when trains are uncoupled and running under ETCS Level 3).

Following trains that are virtually coupled via the V2V channel are considered to form a “convoy”. Trains travelling in a convoy can be separated by a relative braking distance while aiming to form a platoon or can transition to an absolute braking distance separation in case of decoupling for an approaching danger point (e.g., a diverging junction). Two trains travelling in a convoy form a virtually coupled “platoon” when the follower train reaches the speed of the train ahead (i.e., the target speed of its  $EoA_{VC}$ ) at a safe margin (plus buffer time) from this latter, starting to move synchronously with each other, like if they were physically coupled. Trains in a convoy shall be treated as a single train at junctions/stations to ensure route holding, i.e., routes remain locked until the entire convoy has

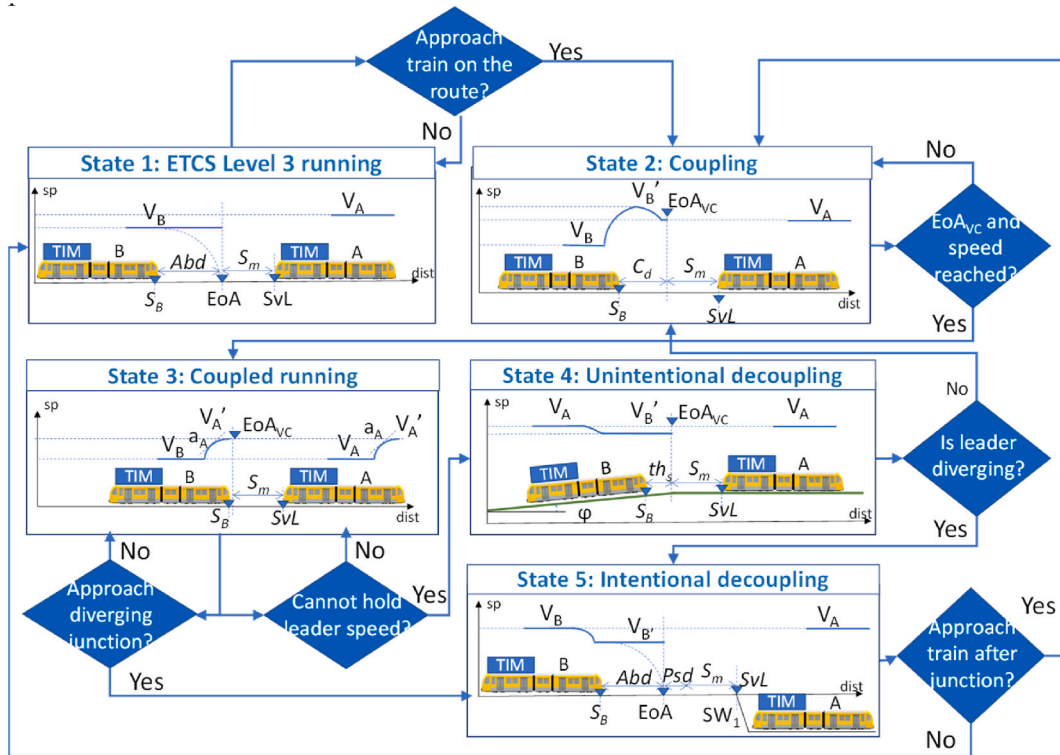


Fig. 2. Flow chart of Virtual Coupling operational states and transitions.

passed.

## 2.2. Modelling of Virtual Coupling railway operations

According to the Institution of Railway Signal Engineers (IRSE 2016) the concept of Virtual Coupling is technologically feasible whereas the main hurdle to its implementation is the definition of principles for safe train distancing in convoys/platoons under disturbed or degraded traffic conditions (e.g., rolling stock breakdown). The EU projects MOVINGRAIL (2020) and X2Rail-3 (2021) have reported that a significant business risk to Virtual Coupling is the rear-end collision in convoys/platoons if one of the leading trains come to a dead stop. A measure to partially mitigate this risk could be adopting the so-called “Running with Emergency Braking Absolute Distance” (REBAD) proposed by Emery (2010) as an additional mode to standard ETCS Level 3. The REBAD mode aims at reducing the risk of rear-end collision of trains travelling at a relative service braking distance by using an absolute emergency braking distance as an additional safety margin. In REBAD mode two trains can be separated by a relative service braking distance ensuring that the follower train always has a full emergency braking distance ahead, to prevent any collision should the leading train suddenly halt. In real-life Virtual Coupling operations, the extra safety margin shall also account for other risk factors depending on V2V communication delays, rolling stock heterogeneity, train positioning errors and extended driving reaction times. Also, the presence of track slopes and train coasting phases might affect the preservation of safe train distancing, especially during platooning operations.

Only limited research has been performed on Virtual Coupling so far and available studies have only partially touched upon the effect of real-life risk factors on safety and capacity. Quaglietta (2019) introduces operational principles for Virtual Coupling to ensure safe train distancing in convoys/platoons on both plain lines and at junctions, developing an infrastructure occupation model to preliminary assess VC capacity gains. The model formulated in Quaglietta (2019) refers however to nominal conflict-free fixed-speed train diagrams which do not consider dynamic interactions among trains. Variable-speed models adjusting train speeds as function of nearby trains' kinematics are hence necessary to reveal the impact of potential risk factors on capacity benefits of Virtual Coupling. Ning (1998) recommends the use of car-following models for the study of Virtual Coupling operations mentioning the need for a safe protection distance which shall be a function of the train service braking rate and the emergency braking rate of the train ahead. Yan et al. (2012) include the safe protection distance suggested by Ning (1998) in a cellular-automata model of train conveying operations for a metro line with homogenous rolling stock. In Pan and Zheng (2014) the safe train distancing for following high-speed trains is a function of the speed differential between leader and follower, which is dynamically controlled to provide a steady speed variation of the follower. Duan et al. (2018) propose an optimised train separation distance by combining moving block with aspects of relative distance braking for trains with homogenous characteristics. Di Meo et al. (2019) define a coupling control algorithm to maintain safe train distancing under Virtual Coupling while accounting for V2V communication delays. Park et al. (2020) develop a robust train

separation controller based on sliding mode control to ensure safe train distancing under Virtual Coupling for homogeneous rolling stock in the presence of speed and position measurement errors. Quaglietta et al. (2020) build a dynamic non-linear multi-state train-following model to describe Virtual Coupling operations, including effects of train stopping patterns, traction power limitations and track gradients for homogeneous trains, using a constant safety margin to make up for position and communication errors. Although all the reported works contribute to a preliminary understanding of Virtual Coupling, none of them investigates the combined effect of realistic railway operation risks on capacity and service performances. To this end, the multi-state train following model by Quaglietta et al. (2020) is extended in this paper by introducing a dynamic safety margin providing safe Virtual Coupling operations under individual or combined risks raised by adverse traffic/infrastructure characteristics or degraded signalling and communication systems.

### 3. A VC multi-state train following model with dynamic safety margin

#### 3.1. Virtual Coupling train-following model description

The model used in this study for describing Virtual Coupling operations draws on the formulation by Quaglietta et al. (2020). Five Virtual Coupling operational states are defined together with corresponding conditions for state transition, as illustrated in the flow chart in Fig. 2. By default, trains are assumed to start operating in a state of “ETCS Level 3 running” (*State 1*). In this state train separation is dynamically supervised by the onboard EVC which imposes an absolute braking distance ( $Abd$ ) before the  $EoA$  located at a safety margin ( $s_m$ ) from the supervised location ( $SvL$ ). The  $SvL$  is represented by a danger point on the route which can be a point or the tail of a train ahead. A train (train B) can transition to a “Coupling” state (*State 2*) when it approaches another one ahead (train A) sharing a portion of route.

The two trains, A and B, link via the V2V channel, forming a convoy in which they start exchanging kinematic information. This information is combined with the standard ETCS  $EoA$  to provide the follower train with a Virtual Coupling End of Authority  $EoA_{VC}$ , having the leader’s speed  $V_A$  as the associated target speed to be attained. Based on the  $EoA_{VC}$  and the speed differential with the leader train, the onboard EVC predicts a coordination distance ( $C_d$ ) necessary to the follower for catching up the leader and achieving its speed ( $V_A$ ) at a safety margin  $s_m$  from this latter’s tail. The coordination distance is defined as  $C_d = t_{coord} \cdot V_A$ , and represents the distance crossed by the leader (moving at speed  $V_A$ ) during the time  $t_{coord}$  required by the follower to reach leader’s speed at the location indicated by the  $EoA_{VC}$  (which is at a  $s_m$  from leader’s tail). If the follower’s speed ( $V_B$ ) is lower than the leader’s,  $t_{coord}$  is simply the time for accelerating to a higher speed ( $V_B'$ ) to catch up with the leader and slowing down to the speed of this latter,  $V_A$ . In the opposite case of the follower’s speed being higher than the leader’s,  $t_{coord}$  is instead the time to brake from  $V_B$  to  $V_A$ . The coordination time  $t_{coord}$ , therefore the corresponding distance  $C_d$  are updated any time speeds and positions of both the leader and the follower trains change according to the formulation reported in Quaglietta et al. (2020) which the interested reader can refer to. A train hence switches from an “ETCS Level 3 running” to a “Coupling” state when the condition  $EoA_{VC} - S_B \leq C_d$  occurs, i.e., when the distance between its front position  $S_B$  and the  $EoA_{VC}$  is not larger than the predicted coordination distance. The follower train successively transitions to a “Coupled running” state (*State 3*) as soon as its speed  $V_B$  nears the leader’s speed  $V_A$  within a certain threshold  $th_v$ , and within a space range  $th_s$  from the  $EoA_{VC}$  (i.e. when  $|V_B - V_A| \leq th_v$  and  $0 \leq S_B - EoA_{VC} \leq th_s$ ). The space and speed thresholds  $th_s$  and  $th_v$  are also called “coupling thresholds”, since their size affects the state transition from “Coupling” to “Coupled running”. When the follower enters a state of “Coupled running” with the leader, the two trains form a virtually coupled platoon in which they move synchronously (i.e., adopting the same speed and acceleration), separated by a safety margin  $s_m$ . From a “Coupled running” state two different transitions might occur leading the platoon to break. The first transition is triggered if the distance between the follower and the leader “unintentionally” exceeds the space threshold  $th_s$  (i.e.,  $EoA_{VC} - S_B \geq th_s$ ) because of excessive motion resistances (e.g. on steep uphill gradients  $\varphi$ ) or limited traction power, which prevent the former to keep the same acceleration of the latter. In this case an “unintentional decoupling” (*State 4*) occurs bringing the follower back to a “Coupling” state where the train aims at catching up the leader again to couple back to it as soon as there are favourable track and traction conditions. The second transition takes place instead when the trains approach a junction where they will diverge over different routes. In that situation, besides the safety margin  $s_m$  the two trains shall be separated by an absolute braking distance  $Abd$  (to allow the follower to safely stop, should the point locking fail) plus the Point switching distance ( $Psd$ ) required to move, set, and lock the point in the correct direction. The Point switching distance is simply the distance crossed by the follower train (approaching the point at speed  $V_B$ ) during the point switching time  $t_{switching}$  (i.e.,  $Psd = V_B \cdot t_{switching}$ ). An “intentional decoupling” (*State 5*) will hence occur when the separation between the follower’s front  $S_B$  and the supervised location of the point  $SvL$  equals the safe separation at the junction  $Abd + Psd + s_m$ , (i.e., if  $SvL - S_B = Abd + Psd + s_m$ ). In a state of “intentional decoupling” the follower train switches back to an “ETCS Level 3 running” imposing again an absolute braking distance between the trains. A state of “intentional decoupling” can however be entered also from an “unintentional decoupling” state whenever a diverging junction is approached.

The description of train motion in each of the defined Virtual Coupling operational states can be obtained by a finite-difference integration of Newton’s motion formula with time step  $\Delta t = t_k - t_{k-1}$ , where  $t_k$  and  $t_{k-1}$  are the current and previous time instant, respectively. If the current operation state  $os_k$  of a train is one among “ETCS Level 3 running”, “Coupling”, “Unintentional decoupling” or “Intentional decoupling”, then the current speed  $v_k$  and position  $s_k$  can be computed as:

$$\begin{cases} v_k = v_{k-1} + \frac{F(v_{k-1}) - R(v_{k-1}, \varphi, r)}{\rho M} \Delta t \\ s_k = s_{k-1} + v_{k-1} \Delta t \end{cases} \quad (1)$$

for  $os_k \in \{\text{State 1, State 2, State 4, State 5}\}$

where  $v_{k-1}$  and  $s_{k-1}$  are the previous train speed and position,  $M$  is the train mass,  $\rho$  the rotating mass factor,  $R$  is the total motion resistance depending on the speed  $v_{k-1}$ , the track gradient  $\varphi$  and the curvature radius  $r$ . The function  $F(v_{k-1})$  denotes the forces applied by the train, which depend on the current driving regime of the train. If a train is accelerating, then the applied force is exclusively the maximum tractive effort  $T(v_{k-1})$ , which is a function of the speed  $v_{k-1}$ . If a train is braking, the force exerted by the train is instead the total braking effort  $\rho \cdot M \cdot b(v_{k-1})$  obtained as the product among the rotating mass factor, the train mass, and the braking rate  $b < 0$  which is a function of the previous speed value  $v_{k-1}$ . If a train is cruising the applied force  $F(v_{k-1})$  equals the total motion resistances  $R(v_{k-1}, \varphi, r)$ , while for a coasting train the applied force is simply zero. Further details about mathematical conditions for transitioning across the various train driving regimes, as well as target speeds,  $EoA$  and  $EoA_{VC}$  locations for the different states, can be found in Quaglietta et al. (2020).

When a train is operating in a state of ‘‘Coupled running’’ and moving synchronously with a train ahead (i.e., the leader) then current speed  $v_k$  and position  $s_k$  are described by the train-following equation:

$$\begin{cases} v_k = v_{k-1} + a_{k-1} \Delta t \\ s_k = s_{k-1} + v_{k-1} \Delta t \end{cases} \quad \text{for } os_k \in \{\text{State 3}\} \quad (2)$$

where the acceleration at the previous time instant  $a_{k-1}$  is the same as the leader  $a_{lead}$ , as long as this latter falls within the range between the maximum  $a_{k-1}^{max}$  and the minimum  $a_{k-1}^{min}$  acceleration actually feasible to the train based on its traction characteristics and maximum braking rate  $b_{max} < 0$ . Train acceleration  $a_{k-1}$  is hence calculated as:

$$a_{k-1} = \begin{cases} a_{k-1}^{max}, & \text{if } a_{lead} > a_{k-1}^{max} = \frac{T(v_{k-1}) - R(v_{k-1}, \varphi, r)}{\rho M} \\ a_{k-1}^{min}, & \text{if } a_{lead} < a_{k-1}^{min} = \frac{\rho M b_{max} - R(v_{k-1}, \varphi, r)}{\rho M} \\ a_{lead}, & \text{otherwise.} \end{cases} \quad (3)$$

### 3.2. Enhancing the train-following model with a dynamic safety margin

The multi-state model developed in Quaglietta et al. (2020) and summarised above refers to a constant safety margin  $s_m$  between the  $EoA_{VC}$  (or the  $EoA$ ) and the supervised location  $SvL$ , for any of the Virtual Coupling states. A constant safety margin is however only acceptable in a perfect theoretical world with no system degradation or failures, whilst it might very likely lead to critical safety violations when considering realistic railway operations. The occurrence of hazards such as train communication delays or extended driving reaction times, may require dynamic adjustments of the safety margin to prevent unsafe overshooting of the  $EoA_{VC}$  or the  $EoA$ , and the consequent collision with the danger point. The multi-state train following model is therefore enhanced by considering a safety margin that varies dynamically over time (hence called dynamic safety margin) depending on train kinematics to compensate for the various risk factors affecting train safety in realistic Virtual Coupling operations. A total of five safety-critical risk factors are identified for VC that need to be tackled by a specific term in the dynamic safety margin. The dynamic safety margin  $dsm_{k,n,n-1}$  at current time  $t_k$  between a train  $n$  and the one ahead  $n - 1$  is hence defined as the sum of five different terms:

$$dsm_{k,n,n-1} = sm_{pos_{k,n,n-1}} + sm_{com_{k,n,n-1}} + sm_{cont_{k,n,n-1}} + sm_{emer_{k,n,n-1}} + sm_0 \quad (4)$$

Each term makes up for a corresponding risk factor, namely: *i*) train positioning errors ( $sm_{pos_{k,n,n-1}}$ ), *ii*) communication update delays ( $sm_{com_{k,n,n-1}}$ ), *iii*) train control delays ( $sm_{cont_{k,n,n-1}}$ ), *iv*) emergency braking application of the leader train ( $sm_{emer_{k,n,n-1}}$ ) and *v*) exogenous factors such as peculiar weather or track conditions that are tackled by a nominal constant safety margin ( $sm_0$ ) which is always imposed between consecutive trains, even when at a standstill.

#### 3.2.1. Train positioning errors

Train location is here assumed to be measured by combining odometry with GNSS systems, which implies that corresponding train positioning errors derive from both devices. According to the ERTMS/ETCS Subset 41 (UNISIG, 2015) the odometry error of a train varies linearly with a slope of 5% along the distance from the last passed balise and it is reset to a maximum error of 5 m as a new reference balise is crossed. The odometry error  $err_{odom_{k,i}}$  of a train  $i$  at current time  $t_k$  is therefore obtained as  $err_{odom_{k,i}} = 5 \pm 5\% \cdot d_{k,i}$ . The variable  $d_{k,i}$  is the distance at time  $t_k$  of train  $i$  from the last relevant balise group, which resets to 0 any time a balise is crossed. The GNSS error  $err_{GNSS_{k,i}}$  of train  $i$  at current time  $t_k$  is instead considered as a constant value ranging from 0 to 20 m depending on the diffraction and/or reflection of the satellite signals over the railway corridor. For any follower-leader couple of trains ( $n, n - 1$ ), the safety margin term  $sm_{pos_{k,n,n-1}}$  at time  $t_k$  shall include the total positioning errors of both trains and can be computed as:

$$sm_{pos_{k,n,n-1}} = \sum_{i=n-1}^n (err_{odom_{k,i}} + err_{GNSS_{k,i}}). \quad (5)$$

**3.2.1.1. Communication update delays.** The exchange of safety-critical information has an update delay time  $\tau_{com}$  representing the actual time necessary for a message to be broadcasted from sender to receiver through a given communication channel. Data sent at time  $t_k$  by the leader train will be received by the follower only at time  $t_k + \tau_{com}$ , i.e., after the communication update delay. For ETCS Level 3 it is here assumed that the updating delay solely affects the train-RBC bidirectional communication, while for VC an additional communication delay is considered to exchange train kinematics via the V2V channel. No safety issue arises if the leader train runs faster than the follower since the train separation will progressively increase. If the leader is instead running slower than the follower, then an additional safety margin is needed to make up for the larger distance covered by the follower within the communication delay, which unsafely shortens the train separation. To mitigate potential safety risks due to the communication delay, the term  $sm_{com_{k,n,n-1}}$  needs to be added at time  $t_k$  to the safety margin between train  $n$  and its leader  $n - 1$ . This term is expressed as:

$$sm_{com_{k,n,n-1}} = \max(0, \tau_{com} v_{k,n} - \tau_{com} v_{k-c,n-1}) \quad (6)$$

where  $v_{k,n}$  is the current speed of the follower,  $v_{k-c,n-1}$  is the speed broadcasted by the leader before the communication update delay and  $c = \tau_{com}/\Delta t$ , with  $\Delta t$  the integration step.

### 3.2.2. Train control delays

Whenever safety-critical data is received by a train (e.g., a signal aspect, MA or  $MA_{VC}$ ), a certain time  $\tau_c$  (called control delay) is always needed to convert that data into a corresponding action to safely control the train. On railway lines with conventional fixed-block multi-aspect signalling and human driver, the control delay is simply the time for the driver to see the aspect of the approaching signal and react to it by braking or traction. Similarly, for driverless trains under Virtual Coupling the control delay is the time for the automatic train operation to compute and implement a suitable acceleration/braking command enabling a train to follow, couple to or decouple from a train ahead. If a train has a shorter control delay than the one ahead then there are no safety concerns. Train separation can instead dangerously shorten when the control delay  $\tau_{c,n}$  of a follower train  $n$  is larger than the control delay  $\tau_{c,n-1}$  of its leader  $n - 1$ . In that case, an additional safety margin  $sm_{cont_{k,n,n-1}}$  needs to be added at current time  $t_k$ , which is computed as:

$$sm_{cont_{k,n,n-1}} = \max(0, \tau_{c,n} \cdot v_{k,n} - \tau_{c,n-1} \cdot v_{k-c,n-1}), \quad (7)$$

where  $v_{k,n}$  is the current speed of the follower,  $v_{k-c,n-1}$  is the last speed information sent by the leader before the communication update delay, and  $c = \tau_{com}/\Delta t$ , with  $\Delta t$  the integration step.

### 3.2.3. Emergency braking applications of the leader

When moving in a Virtual Coupling convoy trains are separated by less than an absolute braking distance, which is an unsafe condition should a train ahead suddenly apply an emergency braking. As suggested by Emery (2010) an extra safety margin can be added corresponding to the difference between the service braking distance of the follower and the emergency braking distance of the leader. In this way the follower can apply a service braking to safely stop in rear of the leader if this latter has halted in an emergency. To prevent any collision between the follower  $n$  and the leader  $n - 1$ , the additional safety margin  $sm_{merk_{n,n-1}}$  is required at current time  $t_k$ , which is expressed as:

$$sm_{merk_{n,n-1}} = \max\left(0, \frac{(v_{k,n})^2}{2b_n} - \frac{(v_{k-c,n-1})^2}{2b_{merk_{n-1}}}\right), \quad (8)$$

where  $v_{k,n}$  and  $b_n$  are the current speed and the service braking rate of the follower while  $v_{k-c,n-1}$  (with  $c = \tau_{com}/\Delta t$ ) and  $b_{merk_{n-1}}$  are the last transmitted speed information and the emergency braking rate of the leader, respectively. Therefore,  $sm_{merk_{n,n-1}}$  is obtained by subtracting the emergency braking distance of the leader from the service braking distance of the follower if this is bigger than zero.

### 3.2.4. Exogenous factors

External factors such as weather or track conditions might adversely affect the safe train separation. To mitigate the risk raised by those factors an additional constant safety margin  $sm_0$  is imposed between two consecutive trains. This means that even if the trains are stopped or there is no other risk factor, trains will always be separated by at least the margin  $sm_0$ . This term coincides with the only safety margin accounted for Virtual Coupling in Quaglietta et al. (2020) where purely theoretical and perfect operational conditions were assumed.

The defined dynamic safety margin is hence used to compute the  $EoA_{VC}$  for a train moving under Virtual Coupling. The enhanced train-following model is simply obtained by substituting the constant safety margin  $s_m$  with the dynamic safety margin  $ds_{m_{k,n,n-1}}$  to all state transition conditions and motion equations given in Section 3.1. Specifically, when trains operate under ETCS Level 3 supervision the dynamic safety margin will not include the terms to make up for emergency braking applications of the leader (given the absolute braking distance separation) and the V2V communication delays (since only the train-RBC communication delay is present). For all the other Virtual Coupling operational states the dynamic safety margin is instead composed of all the defined terms.



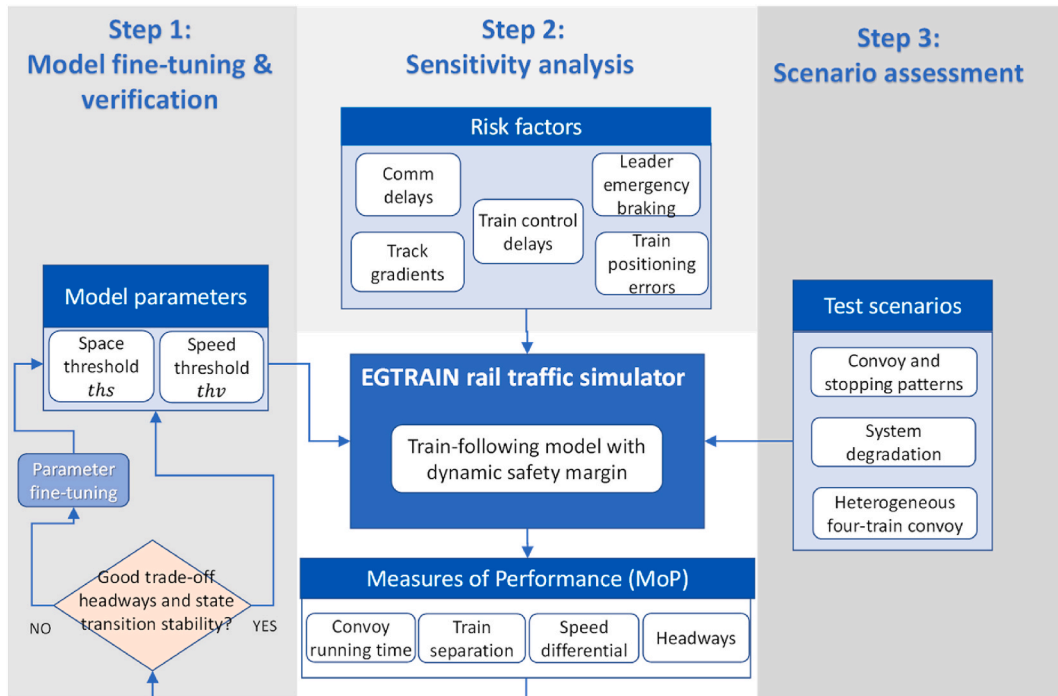


Fig. 3. Three-step analysis framework to analyse realistic Virtual Coupling operations.

#### 4. Three-step analysis of realistic Virtual Coupling operations

A three-step approach (Fig. 3) is used to analyse the implications that Virtual Coupling could have on train dynamics and network capacity when realistic risk factors and operational scenarios are considered. To perform the analysis, the developed train-following model is embedded in the microscopic time-driven rail traffic simulation tool EGTRAIN (Quaglietta 2014).

Rolling stock, train services, infrastructure and signalling characteristics are described at high level of detail in EGTRAIN, allowing for an accurate description of train dynamics. Additionally, both fixed-block and moving-block signalling can be simulated thereby enabling a capacity comparison among Virtual Coupling, ETCS Level 3 moving-block as well as conventional multi-aspect signalling systems (e.g., the British TPWS with 4-aspect signalling).

Several Measures of Performance (MoP) are used to assess network capacity and train dynamics under Virtual Coupling, namely: the separation distance, the time headway, the speed differential, and the convoy running time intended as the total time two trains run as a convoy. The convoy running time is obtained by summing the time spent by the follower train in both the states of “coupling” and “coupled running”.

##### Step 1: Model fine-tuning.

In the first step (Step 1) of the analysis, the multi-state train-following model is fine-tuned. The space ( $th_s$ ) and speed ( $th_v$ ) thresholds are tuned one-by-one until the model reproduces a stable behaviour without unnecessary state transitions of the follower while keeping headways as low as possible. Small values of  $th_s$  and  $th_v$  could lead to switch from a state of “coupled running” to “unintentional decoupling” by the follower train at slight speed or distance deviations from the thresholds, consequently increasing train headways. For relatively large space and speed thresholds it might instead happen that the model forces the follower train to stay in a “coupled running” state even when motion resistances or traction power prevent keeping leader’s accelerations. This also leads to increased train separations (and headways) since the follower train would take longer to switch to an “unintentional decoupling” state and catch up the train ahead.

##### Step 2: Sensitivity analysis.

The second step (Step 2) investigates the sensitivity of network capacity to the various risk factors existing in realistic Virtual Coupling train operations. The risk factors accounted for as input parameters to the train-following model are: V2V communication delays, extended ATO reaction times, train positioning errors, emergency brake applications of the train ahead, and heterogeneity of operating traffic. Also, the sensitivity to track gradients is studied, since the possibility of trains to travel in platoons can be influenced by the track elevation profile.

A One-At-a-Time (OAT) sensitivity analysis is implemented where each of the different risk factors as input to the model, is changed one by one while leaving the others fixed at a certain value. Specifically, the Morris screening method as enhanced by Campolongo (2000) is used which computes global sensitivity measures from a set of local elementary effects ( $EE_i$ ) by sampling the  $i$ -th input parameter  $x_i$  over a trajectory traced across the parameter domain. A point  $j$  on a trajectory of parameter  $x_i$  is obtained by changing the

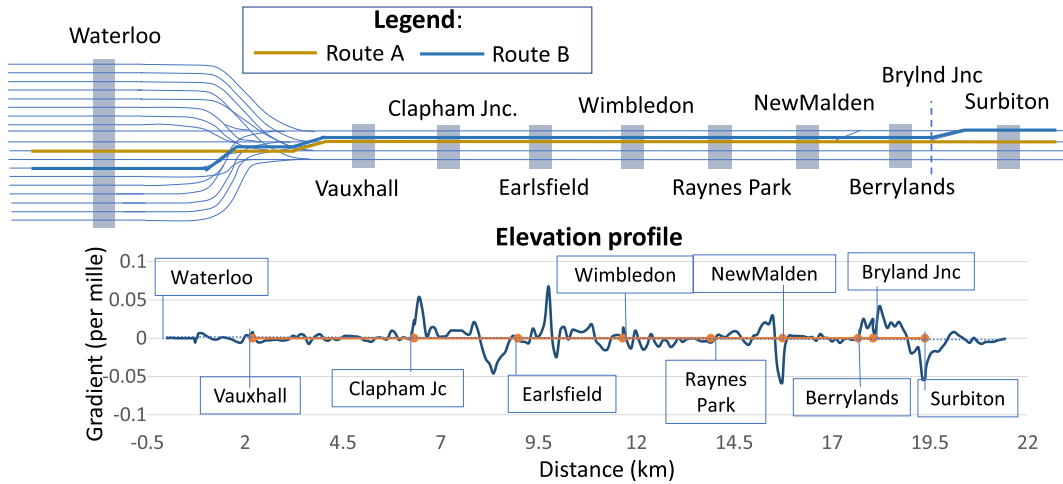


Fig. 4. Track scheme of the Waterloo-Surbiton rail corridor on the South West Main Line.

parameter value by a step  $\Delta_i$ . For a function  $M(x_1, x_2, \dots, x_N)$  with  $N$  input parameters, the elementary effect  $EE_{i,j}$  corresponding to point  $j$  on a trajectory in the space of parameter  $x_i$  is calculated as:

$$EE_{i,j} = \frac{M(x_1, x_2, \dots, x_i + \Delta_i, \dots, x_N) - M(x_1, x_2, \dots, x_i, \dots, x_N)}{\Delta_i} \quad (9)$$

which is basically the average gradient of function  $M$  between two adjacent points  $(x_1, x_2, \dots, x_i + \Delta_i, \dots, x_N)$  and  $(x_1, x_2, \dots, x_i, \dots, x_N)$  on the chosen trajectory for  $x_i$ . The sensitivity of function  $M$  to the  $i$ -th parameter  $x_i$  is then computed as the absolute mean  $\mu_i$  of the elementary effects  $EE_{i,j}$  for  $R$  different points  $j$  on a given trajectory in the parameter space:

$$\mu_i = \frac{1}{R} \sum_{j=1}^R |EE_{i,j}|, \quad (10)$$

as well as the standard deviation of the elementary effects:

$$\sigma_i = \sqrt{\sum_{j=1}^R (EE_{i,j} - \mu_i)^2} \quad (11)$$

Based on the absolute mean and standard deviation of the elementary effects all input parameters can be classified in three groups, namely: inputs with negligible effect, inputs with large linear effects without interactions and inputs with large nonlinear or interaction effect.

In this analysis the sensitivity indexes of the various input factors of the train-following model are calculated with respect to the train headways at a critical location.

The main reasons for using an OAT sensitivity analysis are the computational efficiency (which is linear with the number of model factors) of the method and the independence from the relationship between inputs and outputs of the model. In addition, OAT sensitivity analysis approaches have been largely used for car-following models (e.g., Leclercq et al., 2011), despite their limitation of being unable to capture the effect of combined input variations (Saltelli et al., 2008).

Step 3: Scenario assessment.

The third step (Step 3) investigates the behaviour of the train-following model with dynamic safety margin in several realistic test scenarios including both nominal and degraded traffic conditions. The impact of Virtual Coupling with a dynamic safety margin is assessed in terms of headways and train separations for three different scenarios. The first scenario investigates the effect of possible combinations of train convoy compositions and train stopping patterns. The second scenario analyses two degraded operational conditions, specifically: *i*) a sudden V2V channel degradation which significantly increases the communication latency, and *ii*) an automatic train operation breakdown requiring the handing over to the driver with a consequent extension of train control times. The third scenario pertains instead to nominal traffic conditions where four trains with heterogeneous rolling stock characteristics follow each other in the same convoy. In this latter scenario the distance between first and last train of the convoy is additionally computed and compared to that in ETCS Level 3 moving block as well as to Virtual Coupling with a constant safety margin. Furthermore, the third scenario serves as a test bench to verify the applicability and correctness of the defined train-following model when extended to multiple trains.

**Table 1**  
Rolling stock characteristics of considered train services.

Rolling stock type	Train length [m]	Max speed ( $v_{max}$ ) [m/s]	Service braking rate ( $b$ ) [ $m/s^2$ ]	Emergency braking rate $b_{emerg}$ [ $m/s^2$ ]
BR Class 455	161.84	33.6	0.6	1.2
BR Class 450	163.2	44.7	0.7	1.2
BR Class 220	95	55.8	0.8	1.2

**Table 2**  
Combinations of  $(th_v, th_s)$  tested to fine-tune the VC train-following model.

	$(th_v, th_s)$						
	(1,50)	(1100)	(1200)	(1500)	(2100)	(3100)	(4100)
No. unnecessary transitions	2	0	2	7	2	2	2
Average arrival headway [s]	24	24	27	22	24	23	23

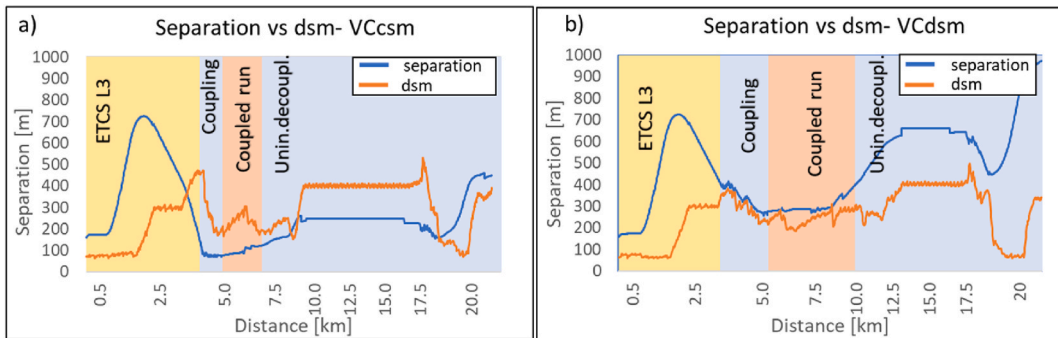


Fig. 5. VC state transitions and separation vs dynamic safety margin for VCdsm.

## 5. Case study application and results

### 5.1. Case study description

The three-step analysis methodology has been applied to the 20 km long corridor between Waterloo and Surbiton on the South West Main Line in the UK (Fig. 4). It has four tracks and a varied elevation profile, becoming very hilly after Clapham Junction.

A mixed-traffic pattern currently operates on the corridor which is relevant to study the effect of heterogeneous train composition on Virtual Coupling operations. Specifically, the analysis refers to three different train service categories, namely: *i*) a suburban service using a British Rail (BR) Class 455, *ii*) a regional service with a BR Class 450 and *iii*) an intercity service served by a BR Class 220. Detailed rolling stock characteristics such as masses, resistance coefficients and tractive effort-speed curves are an input to the EGTRAIN simulation model which has been setup for the analysis.

Some of those characteristics are reported in Table 1 showing for each rolling stock type (first column) the train length (second column), the maximum speed (third column), as well as the service (fourth column) and emergency braking rates (fifth column). As can be seen maximum speeds and service braking rates are larger for the rolling stock used for regional (BR Class 450) and intercity trains (Class 220).

Virtual Coupling operations with a dynamic safety margin are tested and assessed by extensive simulation runs of the enhanced train-following model proposed in this paper. Simulation experiments refer to a nominal operational condition which includes realistic risk factors, namely: a 1 s (second) communication delay, a linear odometry error, a 1 s train control time as well as the chance of emergency braking applications of the leader train. VC with dynamic safety margin ( $VC_{dsm}$ ) is compared to VC operations with the constant safety margin ( $VC_{csm}$ ) defined in Quaglietta et al. (2020). Successively a benchmark is carried out against ETCS Level 3 Moving Block. For all the experiments, both the constant term  $sm_0$  of  $VC_{dsm}$  and the constant margin  $sm$  of  $VC_{csm}$  are set to the same value of 50 m, to keep the comparison consistent. In addition, a temporary speed restriction of 18 m/s is imposed onto the first simulated train just before Clapham junction to allow the trains behind to catch up and couple to it to form a convoy. In real-life rail operations, advanced traffic management algorithms shall instead control train speeds to optimally coordinate the formation/decomposition of Virtual Coupling convoys, especially at junctions and stations.

**Table 3**  
Morris's sensitivity indexes of model parameters for flat track and with gradients.

Input Parameter	Flat track		Track with gradients	
	$\mu_i$	$\sigma_i$	$\mu_i$	$\sigma_i$
Space threshold (m)	0.02	0.00	0.02	0.01
Speed threshold (m/s)	0.00	0.00	0.79	0.25
Position error (m)	0.13	0.22	0.04	0.04
Comm. update delay (s)	1.08	0.17	0.91	0.63
Follower's control delay (s)	1.04	0.07	1.37	0.44
Follower's service braking rate (m/s <sup>2</sup> )	41.33	13.86	49.67	13.25

### 5.2. Model fine-tuning and verification

The VC train-following model with dynamic safety margin is fine-tuned and verified for two suburban trains using the same route in both the scenario of non-stopping and stopping services (at Clapham, Wimbledon, Raynes Park, Surbiton).

The speed and distance thresholds,  $th_v$  and  $th_s$  are fine-tuned to improve the model stability versus unnecessary coupling-decoupling state transitions of the follower and contemporarily keep the average arrival headway (i.e., the station arrival headways averaged across all stations) as low as possible. Several parameter combinations are tested by varying  $th_v$  between 1 m/s and 8 m/s and  $th_s$  between 50 m and 500 m. Table 2 reports (in the second row) the most representative couples ( $th_v$ ,  $th_s$ ) which provided a more stable model behaviour, meaning a reduced number of unnecessary coupling-decoupling transitions (shown in the third row) and a lower average arrival headway (fourth row). As can be seen the couple  $th_v = 1$  m/s and  $th_s = 100$  m (in bold in Table 2) is the one providing the preferred model behaviour with no unnecessary follower's transitions between "coupled running" and "unintentional decoupling" and with a reasonably low average arrival headway. That couple of  $th_v$  and  $th_s$  values are hence set as input to the model for the entire experimental analysis.

The train-following model is then verified by checking that simulated leader-follower separations do not violate the safety margin required in presence of risk factors, i.e., the dynamic safety margin. As part of the verification, the VCdsm model is compared to the VCcsm to capture differences in state transitions of the follower and analyse discrepancies in train separations when risk factors are considered.

Fig. 5 illustrates state transitions of the follower train beside simulated train separations (blue line) and the dynamic safety margin (orange line) for both VCcsm (letter a) and VCdsm (letter b). In presence of risk factors, VCdsm brings to safe train separations never infringing the required dynamic safety margin whereas the VCcsm model unsafely violates the dsm for most of the time. Also, VCcsm allows the trains to form a platoon (i.e. transitioning to "coupled running") much earlier than VCdsm, albeit for a much shorter duration. Using a constant margin in VC hence results into more rigid coupling constraints than using a dynamic one, since being insensitive to leader-follower speed differentials it easily leads to "unintentional decoupling" conditions, whenever the follower cannot longer keep up with the leader.

### 5.3. Sensitivity analysis

A sensitivity analysis of the model has been carried out to investigate the influence of the different input parameters on capacity performances of Virtual Coupling when a dynamic safety margin is adopted.

For each parameter, Morris's sensitivity indexes are computed considering the headways at Surbiton as a measure of service capacity. A total of 64 model evaluations are made by simulating two non-stopping suburban trains Class 450 sharing the same route. To conduct the sensitivity analysis the speed and space thresholds are changed in the range [1 m/s, 8 m/s] and [50 m, 500m], respectively. Train position errors are varied by changing the GNSS error in the range [0 m, 20 m] and by adding to this latter the odometry error as a linear function of the distance from the last crossed balise (see equation (5)). Communication delays and the follower's control delay both range between 1s and 8 s, while the follower's service braking rate varies between 0.4 and 0.9 m/s<sup>2</sup>. When changing one parameter the others are left to the value set in the nominal scenario (as reported in Section 5.1). The influence of track slopes is also analysed by calculating the sensitivity indexes for both a flat track and with the actual track gradients, as reported in Table 3.

The sensitivity results show that the follower's braking rate is by far the most influential parameter to Virtual Coupling capacity. On its own this parameter explains up to 50% (being  $\mu_i = 49.67$ ) of the capacity variance when gradients are considered. The follower's control delays and communication updating times have only a very marginal influence on train separations given that together they explain up to 2.28% (i.e.,  $0.91 + 1.37$ ) of the capacity variance, in case of a sloped track. The speed threshold has only very limited influence when track gradients are considered ( $\mu_i = 0.78$ ) while the space threshold and position errors do not practically affect Virtual Coupling capacity.

### 5.4. Operational scenario 1: convoy composition and stopping pattern

Different convoy compositions and stopping patterns are evaluated to identify operational setups where Virtual Coupling could provide capacity gains over Moving Block. Referring to a scenario with two trains running on the same route, seven different convoy compositions are generated by permutating the sequence "leader-follower" across the three available train categories, i.e., suburban

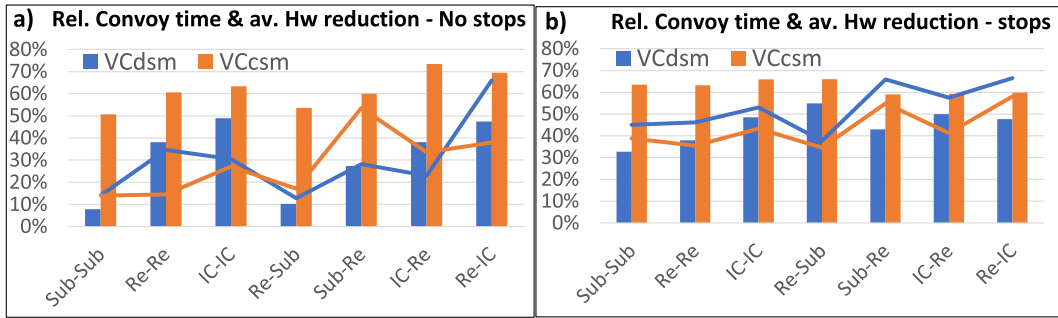


Fig. 6. Relative convoy runtime and average headway reduction for VCdsm and VCcsm.

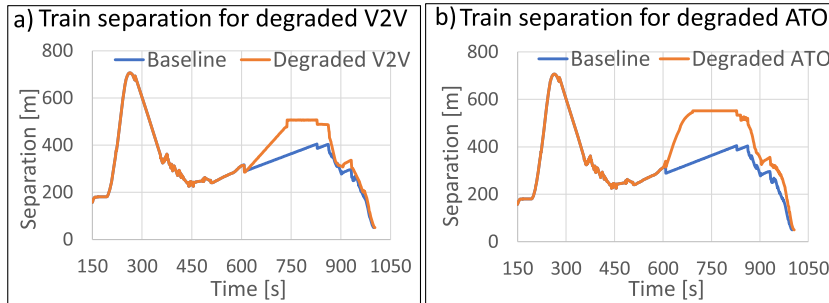


Fig. 7. VCdsm train separation for baseline, degraded V2V (a) and degraded ATO (b).

(Sub), regional (Re) and Intercity (IC). Each convoy composition is then evaluated in the cases of non-stopping and stopping services (with stops at Clapham, Wimbledon, Raynes Park and Surbiton) for ETCS L3, VCdsm and VCcsm. Capacity benefits of VCdsm and VCcsm over ETCS L3 are computed in terms of a “relative average headway reduction” indicator. This latter is simply obtained by calculating the percentage headway reduction of VCdsm (or VCcsm) with respect to ETCS L3 at each station (from Clapham to Surbiton) and then averaging across the number of considered stations. Also, a “relative convoy runtime” indicator is considered, representing the overall time spent by the follower train in both the states of “coupling” and “coupled running” divided by its total running time. Fig. 6 shows a relationship between the relative headway reduction (histograms) and the relative convoy runtime (solid line) for both VCdsm (in blue) and VCcsm (in orange). The general trend is that the higher the convoy running time, the higher is the average headway reduction with respect to moving block. When considering non-stopping services under VCdsm (Fig. 6a), homogeneous convoys provide relevant headway reductions only for trains having better acceleration/braking rates (i.e., IC-IC). For heterogeneous convoys, bigger headway reductions are instead observed when the follower has better acceleration/braking performances than the leader. The term  $sm_{emerk,n,n-1}$  of the dynamic safety margin will be shorter in that case, given the higher braking rate of the follower. Additionally, higher acceleration rates allow the follower to quickly catch up with the leader, thereby shortening the headways. In the opposite case, a follower having worse characteristics than the leader will be more likely to break the convoy by falling into “unintentional decoupling” states from where it will not be able to catch up the leader, if this latter keeps on running at planned speeds. This is observed for the cases Re-Sub and IC-Re, where a VC convoy cannot be kept for long, unless speed restrictions are imposed onto the leader.

When analysing stopping services (Fig. 6b), VCdsm provides average headway reductions beyond 30% for all convoy combinations. Shorter dynamic safety margins are indeed recognised in this case, given the lower speeds attained by trains when approaching stopping stations.

For VCcsm, the relative convoy running time is usually shorter than VCdsm due to more rigid coupling constraints imposed by the constant margin which is insensitive to leader-follower speed differentials. However, greater average headway reductions are observed for all “convoy/stopping patterns” combinations (ranging from 51% to 73.4%) because of the shorter distances at which trains can travel, sometimes resulting in unacceptable infringements of required safe separations.

5.5. Operational scenario 2: system degradation

Two degraded operational scenarios are simulated to investigate the impact of sudden system failures on train separation under VC with dynamic safety margin. Both scenarios refer to an IC following a Regional train with a departure headway of 50 s at Waterloo.

The first degraded scenario assumes a degradation of the V2V channel between Clapham Junction and Earlsfield, which increases the message transfer time by 2s, specifically from 1 s to 3 s (i.e. by 2 s). The second degraded scenario instead supposes that on the same route stretch as the first scenario, the IC’s train driver takes over from the automatic train operation (ATO) because of a

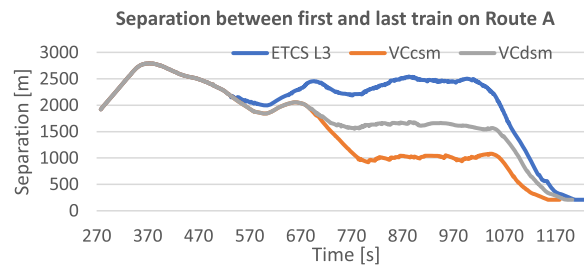


Fig. 8. First and last train separation on Route A for ETCS L3, VCcsm and VCdsm.

malfunctioning. Driving reaction times hence increase from 1 s to 6 s. For both scenarios of a degraded V2V (Fig. 7a) and a malfunctioning ATO (Fig. 7b) an increased train separation (orange line) is observed versus the nominal baseline scenario (blue line) along the degraded portion of route. Specifically, a 2s extension of the communication delay results into a corresponding headway increase of 4s. An extension of the driving reaction time by 5 s increases instead the headway by 6 s. As nominal operational conditions are restored, the follower catches up the leader again, progressively bringing back the separation to the nominal safe distance of the baseline.

The VC train-following model with dynamic safety margin hence correctly reacts to system degradations by increasing train separations to guarantee necessary safety distances for as long as needed.

### 5.6. Operational scenario 3: four-train heterogeneous train convoy

A further operational scenario with four heterogeneous trains is considered to study both the applicability of the VC train-following model and train dynamics for a heterogeneous convoy composed of more than two trains. The first train is a suburban Class 455 train, the second is a regional Class 450, the third one an Intercity Class 220 while the fourth is again a regional train Class 450. All trains depart from Waterloo with a headway of 50 s. The first two trains operate on Route A (Fig. 4) while the last two on Route B, meaning that these latter will detach from the convoy and diverge at Berryland Junction. A temporary speed restriction of 65 km/h is imposed to the first train over the initial 4.70 km of its route to allow the following trains to catch up with it and form a convoy. Capacity impacts of VC with dynamic safety margin are computed in terms of head-to-head separation between the first and the last train on Route A (that for VC is the convoy length on Route A).

As illustrated in Fig. 8 the separation obtained for VCdsm (grey line) is then compared with that obtained for ETCS Level 3 (blue line) and VCcsm (orange line). In the initial part of the route the first-last train separation for VCcsm and VCdsm coincides with that of ETCS L3 since trains are all in a state of “ETCS Level 3 running”. As they start forming a convoy the separation drops until the four trains form a virtually coupled platoon for which the separation stabilises around a constant value (represented by the approximate horizontal leg of the grey and orange lines). In platooning, VCcsm is able to reduce the ETCS L3 distance between first and last train from 2515 m to 1044 m (−59%) while VCdsm brings that down to 1671 m (−34%). Note that for a physical coupling the distance would be 420 m between the heads of the first and fourth train, although these different train classes cannot be physically coupled. When trains approach Berryland Junction (around 980–1000 s) the train separation increases, since the last two trains slow down until an absolute braking distance is achieved before the junction to safely diverge over Route B. After the diverging junction, only the first two trains will remain on route A which explains the sudden drop in the separation between the first and last train for both VC and ETCS L3. When approaching Surbiton, the separation between the two trains on Route A further decreases (due to the speed reduction before stopping) until reaches a constant value of 212 m at the stop, which equals the length of the first train plus the 50 m margin  $sm_0$ . A general result is that VCcsm leads to very short but often unsafe separations between the first and the last train. Instead, VCdsm provides separations which are still substantially shorter than ETCS Level 3 while respecting necessary safety distances between any leader-follower couple in the convoy.

## 6. Conclusions

This paper analyses train dynamics and capacity impacts of Virtual Coupling signalling when considering risk factors in real-life operations such as train communication delays, extended reaction times, emergency braking applications and traffic heterogeneity. The concept of dynamic safety margin is introduced for Virtual Coupling which dynamically varies train separations to prevent safety violations in hazardous events (e.g., V2V communication delays). A mathematical representation of the dynamic safety margin is formulated and integrated with the multi-state VC train-following model by Quaglietta et al. (2020) which originally referred to a constant safety margin, hence insensitive to real-life operational risks. A three-step methodology framework is applied to the case of the South West Main Line in the UK, to verify and analyse the model as well as assess VC operations under different scenarios. In the first step the train-following model is fine-tuned and successfully verified by checking that simulated train separations always respect minimum safety margins in presence of operational risk factors. In the second step, an OAT sensitivity analysis shows that Virtual Coupling capacity performances are mostly affected by the risk of emergency braking applications of the leader train whereas only little influence have delays in train communication and control. In the third step, three operational scenarios are analysed. The first

scenario investigates the effect of heterogeneous convoy compositions and stopping patterns on VC capacity. Outcomes show that for non-stopping services VC with dynamic safety margin provides capacity gains over ETCS Level 3 moving block when a train is followed by one with better acceleration/braking characteristics (e.g., a Regional followed by an Intercity). For stopping services capacity gains are instead obtained for any type of train following another. The second operational scenario illustrates that in case of sudden failures of the V2V communication channel or the ATO, VC operations with a dynamic safety margin increase the train separation to a safe distance until nominal conditions are restored. The third scenario investigates Virtual Coupling train interactions for a heterogeneous four-train convoy, showing that the use of a dynamic safety margin can substantially reduce train separations with respect to ETCS Level 3 moving block. Future research will be devoted to defining a more detailed modelling of the V2V communication layer which here is assumed not to be constrained by a specific distance range. Also, the coupling parameters will be calibrated to maximise the driving stability of the follower train. Additional studies will be looking at optimised train control strategies to optimally form/split convoys over the network so to maximise capacity.

## Data availability

Data will be made available on request.

## References

- Campolongo, F., Kleijnen, J., Andres, T., 2000. Screening methods. In: Saltelli, A., Chan, K., Scott, E.M. (Eds.), *Sensitivity Analysis*. Wiley, Chichester, pp. 65–80.
- Di Meo, C., Di Vaio, M., Flammini, F., Nardone, R., Santini, S., Vittorini, V., 2019. ERTMS/ETCS virtual coupling: proof of concept and numerical analysis. *IEEE Trans. Intell. Transport. Syst.* 21 (6), 2545–2556.
- Duan, H., Schmid, F., 2018. Optimised headway distance moving block with capacity analysis. In: *Proceedings of the IEEE International Conference on Intelligent Rail Transportation (ICIRT)*, pp. 1–5.
- Emery, D., 2010. Enhanced ETCS L2/L3 train control system. In: *WIT Transactions on State-of-the-art in Science and Engineering*, 46, pp. 112–122.
- IRSE International Technical Committee, 2016. ERTMS Level 4, Train Convoys or Virtual Coupling-Report on Topic 39, vol. 219. IRSE News, pp. 1–3.
- Leclercq, L., Laval, J.A., Chiabaut, N., 2011. Capacity drops at merges: an endogenous model. *Procedia Soc. Behav. Sci.* 17, 12–26.
- MOVINGRAIL, 2020. (MOVing block and VIRTual coupling New Generations of RAIL signalling) available at: <https://movingrail.eu/>. last accessed on December, the 8th, 2020.
- Ning, B., 1998. Absolute braking and relative distance braking – train operation control modes in moving block systems. *Trans. Built Environ.* 34, 991–1001.
- Pan, D., Zheng, Y., 2014. Dynamic control of high-speed train following operation. *Promet - Traffic & Transp.* 26 (4), 291–297.
- Park, J., Lee, B.H., Eun, Y., 2020. Virtual coupling of railway vehicles: gap reference for merge and separation, robust control, and position measurement. *IEEE Trans. Intell. Transport. Syst.* 1–12, 10.1109/TITS.2020.3019979.
- Quaglietta, E., 2014. An approach to design the layout of railway signaling system to maximize the economic efficiency of the network. *Simulat. Model. Pract. Theor.* 46, 4–24.
- Quaglietta, E., 2019. Analysis of Platooning Train Operations under V2V communication-based signalling: fundamental modelling and capacity impacts of Virtual Coupling. In: *Proceedings of the 98<sup>th</sup> Transportation Research Board Annual Meeting, Washington DC, 13<sup>th</sup>-17<sup>th</sup> January 2019*.
- Quaglietta, E., Wang, M., Goverde, R.M.P., 2020. A multi-state train-following model for the analysis of virtual coupling railway operations. *J. Rail Trans. Plann. Manag.* 15.
- Saltelli, A., Ratto, M., Andres, T., Campolongo, F., Cariboni, J., Gatelli, D., Tarantola, S., 2008. *Global Sensitivity Analysis: the Primer*. John Wiley & Sons.
- Shift2Rail Joint Undertaking, 2015. Shift2Rail Multi-Annual Action Plan. available online at: Brussels. [https://www.shift2rail.org/wp-content/uploads/2013/07/MAAP-final\\_final.pdf](https://www.shift2rail.org/wp-content/uploads/2013/07/MAAP-final_final.pdf).
- Theeg, G., Vlasenko, S., 2009. *Railway Signalling & Interlocking: International Compendium*, Eurailpress. Hamburg.
- UNISIG, 2015. SUBSET-041 (v3.2.0) - ERTMS/ETCS - Performance Requirements for Interoperability - X2Rail-3, 2021. last accessed, February 3rd. [https://projects.shift2rail.org/s2r\\_ip2\\_n.aspx?p=X2RAIL-3](https://projects.shift2rail.org/s2r_ip2_n.aspx?p=X2RAIL-3).
- Yan, X., Cheng-Xun, C., Ming-Hua, L., Jin-Long, L., 2012. Modeling and simulation for urban rail traffic problem based on cellular automata. *Commun. Theor. Phys.* 58 (6), 847–855.